European Journal of Mechanics B/Fluids 34 (2012) 91–96

Contents lists available at SciVerse ScienceDirect

European Journal of Mechanics B/Fluids

journal homepage: www.elsevier.com/locate/ejmflu

# An exact solution of AC electro-kinetic-driven flow in a circular micro-channel

Ali Jabari Moghadam *

*Department of Mechanical Engineering, Shahrood University of Technology, Shahrood, Iran*

ARTICLE INFO

*Article history:*
Received 5 July 2011
Received in revised form
2 January 2012
Accepted 6 March 2012
Available online 17 March 2012

*Keywords:*
Micro-fluidics
AC electro-kinetic-driven flow
Navier–Stokes equations
Circular micro-channel
Analytical solution
Frequency

ABSTRACT

The electro-osmotic fully-developed flow in a circular micro-channel is studied under an alternating electrical field. An analytical approach based on the linearized Poisson–Boltzmann equation is selected to get an exact solution of the electrical potential inside the channel. An exact solution of the velocity distribution is then obtained by using the Green's function approach. The application of the electrical body force results in a rapid acceleration of the fluid within the double layer. If the diffusion time scale is much greater than the oscillation period (high frequency), the fluid within the double layer oscillates rapidly, while the bulk fluid remains almost stationary.



## 1. Introduction

In recent years, considerable progress has been made in the field of miniaturization. It is now effectively possible to miniaturize all kinds of systems—e.g., mechanical fluidic, electromechanical, or thermal-down to sub-micrometric sizes. In particular, the micro-fluidic systems have been developed in which a fluid circulates inside a miniaturized channel, named micro-channel, by applying an electrical field along it. The rapid expansion of the micro-fluidics field seems to be driven in part by the possibility of integration. The domain of integrated analysis systems has been designated as micro-total analysis systems, or also lab-on-a-chip systems. Generally, a lab-on-a-chip device has a network of micro-channels, electrodes, sensors and electrical circuits. The advantages of these labs on a chip include dramatically reduced sample size, much shorter reaction and analysis time, high throughput, automation and portability [1]. The electro-osmotic flow is usually preferred over the pressure-driven flow, because pumping a liquid through a very small channel requires applying very large pressure difference depending on the flow rate. Additionally, it does not require any external pump, but needs electrodes to control the flow field.

Among the researchers that worked on these phenomena, Anderson [2] studied the particle movement produced by non-uniform zeta potential in an electric field. The effect of inhomogeneously charged surfaces on electro-osmosis was reported by Ajdari [3]. Wang and Chen [4] investigated electro-osmosis in homogeneously charged micro- and nanoscale random porous media using mesoscopic simulation methods which involve a random generation-growth method for reproducing three-dimensional random micro-structures of porous media and a lattice Poisson–Boltzmann algorithm for solving the strongly nonlinear governing equations. Wang et al. [5] modeled physicochemical transport due to electro-osmosis of dilute electrolyte solutions through micro-porous media with granular random microstructures by a three-step numerical framework. They investigated the effects of porosity, ionic concentration, pH, and temperature on the electro-osmotic permeability through the granular micro-porous media.

Among the researchers that worked on DC electro-osmotic flows, Dutta and Beskok [6] presented analytical results for velocity distribution, mass flow rate, pressure gradient, wall shear stress, and vorticity in mixed electro-osmotic/pressure driven flows for two-dimensional straight channel geometry. Arulanandam and Li [7] studied the liquid movement in a rectangular micro-channel by electro-osmotic pumping. Soong and Wang [8] studied flow and heat transfer between two parallel plates.

AC electro-osmotic flows have been studied by some researchers. Among them, Kang et al. [9] solved the electro-osmotic flow problem in a cylindrical channel for only sinusoidal waveform by the Green's function method. Wang and Kang [10] presented a numerical solution based on coupled lattice Boltzmann methods for electro-kinetic flows in micro-channels. They also presented an analytical flow field model, based on a surface slip condition approach, for an axially applied AC electrical field in an infinitely wide micro-channel. Comprehensive models for such a slit channel have also been presented by Dutta and Beskok [11] who developed

* Fax: +98 273 3395440.
*E-mail addresses:* jm.ali.project@gmail.com, jabariali@rocketmail.com.

0997-7546/$ – see front matter © 2012 Elsevier Masson SAS. All rights reserved.
doi:10.1016/j.euromechflu.2012.03.006

an analytical model for an applied sinusoidal electric field, and Soderman and Jonsson [12] who examined the transient flow field caused by a series of different pulse designs. Erickson and Li [13] presented a combined theoretical and numerical approach to investigate the time periodic electro-osmotic flow in a rectangular micro-channel.

As an alternative to traditional DC electro-osmosis, a series of novel techniques have been developed to generate bulk flow using AC fields. For example, Green et al. [14] experimentally observed peak flow velocities on the order of hundreds of micrometers per second near a set of parallel electrodes subject to two AC fields, 180° out-of-phase with each other. The effect was subsequently modeled using a linear double layer analysis by Gonzalez et al. [15]. Using a similar principle, both Brown et al. [16] and Studer et al. [17] presented micro-fluidic devices that incorporated arrays of non-uniformly sized embedded electrodes which, when subject to an AC field, were able to generate a bulk fluid motion.

In this research, an exact solution of flow induced by unsteady applied electric fields inside a circular micro-channel has been developed. The closed-form solution of the momentum equation presented within the Debye–Huckel approximation can be used to get the velocity profiles due to applying any time-periodic electric fields. This kind of micro-channel with its particular applied electric field has its unique features and applications. Lab-on-a-chip devices having networks of micro-channels are miniaturized bio-medical or chemistry laboratories on a small glass or plastic chip. Applying electrical fields along micro-channels controls the liquid flow and other operations in the chip. These labs on a chip can duplicate the specialized functions as their room-sized counterparts, such as clinical diagnostics, DNA scanning and electro-phoretic separation.

## 2. Problem formulation

Consider a fully-developed flow inside a circular micro-channel that is produced by an electric field in the absence of any pressure gradients.

First of all, we must know the local net charge density per unit volume $\rho_e$ at any point in the solution. This requires solving the EDL field [18]:

$$\nabla^2\psi = \frac{2\mathbb{Z}en_0}{\varepsilon}\sinh\left(\frac{\mathbb{Z}e\psi}{k_BT}\right) \tag{1}$$

where, $\psi$ is the electrical potential.

For pure electro-osmotic fully-developed flows of incompressible fluids in circular micro-channels, the Navier–Stokes equations take the following form [19]:

$$\rho\frac{\partial V_z}{\partial t} = \mu\left(\frac{\partial^2 V_z}{\partial r^2} + \frac{1}{r}\frac{\partial V_z}{\partial r}\right) - \rho_e E(\omega t) \tag{2}$$

where, $V_z$ is the only non-zero velocity component along the channel, $\rho$ and $\mu$ are the density and the viscosity of liquid, respectively, and $E(\omega t)$ is a general time-periodic function with a frequency $\omega = 2\pi f$ that describes the applied electric field strength.

Eqs. (1) and (2) are the governing equations of this problem. The boundary conditions are:

$$\begin{cases} r = 0 : \dfrac{d\psi}{dr} = 0 \\ r = \Re : \psi = \zeta \end{cases} \tag{3}$$

$$\begin{cases} r = 0 : \dfrac{\partial V_z}{\partial r} = 0 \\ r = \Re : V_z = 0 \end{cases} \tag{4}$$

where, $\Re$ and $\zeta$ are the channel radius and the zeta potential, respectively.

Consider the following dimensionless variables:

$$R = \frac{r}{\Re}, \qquad \Psi = \frac{\mathbb{Z}e}{k_BT}\psi, \qquad \theta = \frac{\mu}{\rho\Re^2}t,$$
$$\Omega = \frac{\rho\Re^2}{\mu}\omega, \qquad V = \frac{\mathbb{Z}e\mu}{\varepsilon E_z k_B T}V_z \tag{5}$$

in which, $E_z$ is a constant equivalent to the strength of the applied electric field. Introducing the above dimensionless variables into Eqs. (1) and (2) gives the following non-dimensional forms of the governing equations:

$$\nabla^2\Psi = (\kappa\Re)^2\sinh\Psi \tag{6}$$

$$\frac{\partial V}{\partial\theta} = \frac{\partial^2 V}{\partial R^2} + \frac{1}{R}\frac{\partial V}{\partial R} + (\kappa\Re)^2\sinh\Psi\, F(\Omega\theta) \tag{7}$$

where, $F(\Omega\theta)$ is a general periodic function of unit magnitude such that $E(\Omega\theta) = E_z F(\Omega\theta)$. $\kappa$ is the Debye–Huckel parameter defined as follows:

$$\kappa = \left(\frac{2\mathbb{Z}^2e^2n_\infty}{\varepsilon\varepsilon_0 k_BT}\right)^{1/2}. \tag{8}$$

The boundary conditions (3) and (4) also take the following dimensionless form:

$$\begin{cases} R = 0 : \dfrac{d\Psi}{dR} = 0 \\ R = 1 : \Psi = Z \end{cases} \tag{9}$$

$$\begin{cases} R = 0 : \dfrac{\partial V}{\partial R} = 0 \\ R = 1 : V = 0. \end{cases} \tag{10}$$

Eq. (6), under the condition that the double layer potential $\Psi$ is small, can be linearized by the so-called Debye–Huckel approximation, yielding:

$$\frac{d^2\Psi}{dR^2} + \frac{1}{R}\frac{d\Psi}{dR} = K^2\Psi \tag{11}$$

in which, the constant $K$ has been introduced to denote $\kappa\Re$ (electro-kinetic radius). The solution of (11) subject to the boundary conditions (9) is:

$$\Psi(R) = \frac{Z}{I_0(K)}I_0(KR) \tag{12}$$

where, $I_\nu(x)$ is the modified Bessel function of the first kind and order $\nu$, satisfying the following modified Bessel function:

$$x^2y'' + xy' - \left(x^2 + \nu^2\right)y = 0. \tag{13}$$

In order to solve Eq. (7), the Debye–Huckel approximation is implemented to result in the following form of the equation:

$$\frac{\partial V}{\partial\theta} = \frac{\partial^2 V}{\partial R^2} + \frac{1}{R}\frac{\partial V}{\partial R} + \underbrace{K^2\Psi(R)F(\Omega\theta)}_{Q(R,\theta)}. \tag{14}$$

A Green's function approach is now used to find an analytical solution for the non-dimensional form of the motion Eq. (14). The Green's function and the boundary conditions become [20]:

$$\frac{\partial g}{\partial\theta} - \frac{1}{R}\frac{\partial}{\partial R}\left(R\frac{\partial g}{\partial R}\right) = \frac{\delta(R-\ell)\,\delta(\theta-\tau)}{2\pi R} \tag{15}$$

$$\begin{Bmatrix} \lim\limits_{R\to 0}|g(R,\theta;\ell,\tau)| < \infty \\ g(1,\theta;\ell,\tau) = 0 \end{Bmatrix}, \quad 0 < R,\ \ell < 1,\ 0 < \theta, \tau \tag{16}$$

where, $\delta(x)$ is Dirac delta function. We begin by taking the Laplace transform (15):

$$\frac{1}{R}\frac{d}{dR}\left(R\frac{dG}{dR}\right) - sG = \frac{-e^{-s\tau}}{2\pi R}\delta\left(R-\ell\right). \tag{17}$$

Next we re-express $\frac{\delta(R-\ell)}{R}$ as the Fourier–Bessel expansion:

$$\frac{\delta\left(R-\ell\right)}{2\pi R} = \sum_{n=1}^{\infty} A_n J_0\left(\lambda_n R\right) \tag{18}$$

where, $\lambda_n$ is the nth root of $J_0(\lambda) = 0$, and, $J_\nu(x)$ is the Bessel function of the first kind and order $\nu$. Also, we have:

$$A_n = \frac{2}{J_1^2\left(\lambda_n\right)}\int_0^1 \frac{\delta\left(R-\ell\right)}{2\pi R} J_0\left(\lambda_n R\right) R dR = \frac{J_0\left(\lambda_n R\right)}{\pi J_1^2\left(\lambda_n\right)}. \tag{19}$$

So that,

$$\frac{1}{R}\frac{d}{dR}\left(R\frac{dG}{dR}\right) - sG = -\frac{e^{-s\tau}}{\pi}\sum_{n=1}^{\infty}\frac{J_0\left(\lambda_n\ell\right)J_0\left(\lambda_n R\right)}{J_1^2\left(\lambda_n\right)}. \tag{20}$$

The solution to (20) is:

$$G\left(R, s; \ell, \tau\right) = \frac{e^{-s\tau}}{\pi}\sum_{n=1}^{\infty}\frac{J_0\left(\lambda_n\ell\right)J_0\left(\lambda_n R\right)}{\left(s+\lambda_n^2\right)J_1^2\left(\lambda_n\right)}. \tag{21}$$

Taking the inverse of (21) and applying the second shifting theorem gives:

$$g\left(R, \theta; \ell, \tau\right) = \frac{H\left(\theta-\tau\right)}{\pi}\sum_{n=1}^{\infty}\frac{J_0\left(\lambda_n\ell\right)J_0\left(\lambda_n R\right)}{J_1^2\left(\lambda_n\right)}e^{-\lambda_n^2(\theta-\tau)} \tag{22}$$

in which, $H(x)$ is the Heaviside step function.

To find the velocity, we use the following simplified formula, subject to the homogeneous boundary conditions discussed above:

$$V\left(R,\theta\right) = \int_0^\theta\int_0^1 g\left(R,\theta;\ell,\tau\right)Q\left(\ell,\tau\right)\,d\ell d\tau. \tag{23}$$

Now, two different periodic functions are examined; the first is a sinusoidal function, and the other is a square wave function.

If the periodic function is $F(\Omega\theta) = \sin(\Omega\theta)$, taking the above integrals will give the non-dimensional velocity profile which is given in Box I. And if the following periodic square wave is applied:

$$F\left(\Omega\theta\right) = \frac{2}{\pi}\sum_{m=1}^{\infty}\frac{1-\cos\left(m\pi\right)}{m}\sin\left(m\Omega\theta\right) \tag{25}$$

the non-dimensional velocity profile will be as follows:

$$\begin{aligned} V&\left(R,\theta\right) \\ &= \frac{2K^2Z}{\pi^2 I_0(K)}\sum_{n=1}^{\infty}\sum_{m=1}^{\infty}\times\frac{J_0\left(\lambda_n R\right)}{mJ_1^2\left(\lambda_n\right)\left(\lambda_n^4+m^2\Omega^2\right)} \\ &\quad\times\left(\int_0^1 J_0\left(\lambda_n\ell\right)I_0\left(K\ell\right)d\ell\right) \\ &\quad\times\left[m\Omega\left(-\cos\left(m\Omega\theta\right)+e^{-\lambda_n^2\theta}+\cos\left(m\pi\right)\cos\left(m\Omega\theta\right)\right.\right. \\ &\quad\left.\left.-\cos\left(m\pi\right)e^{-\lambda_n^2\theta}\right)+\lambda_n^2\sin\left(m\Omega\theta\right)\left(1-\cos\left(m\pi\right)\right)\right]. \end{aligned} \tag{26}$$

The integrals containing Bessel functions in Eqs. (24) and (26) can be simply determined by the following series with good accuracy:

$$\begin{aligned} &\int_0^1 J_0\left(\lambda_n\ell\right)I_0\left(K\ell\right)d\ell \\ &\cong 1+\frac{1}{12}\left(K^2-\lambda_n^2\right)+\frac{1}{320}\left(K^4+\lambda_n^4\right)-\frac{1}{16128}\left(K^6-\lambda_n^6\right) \\ &\quad+\frac{1}{1327104}\left(K^8+\lambda_n^8\right)-\frac{1}{80}\lambda_n^2K^2+\frac{\lambda_n^2K^2}{1792}\left(\lambda_n^2-K^2\right) \\ &\quad-\frac{\lambda_n^2K^2}{82944}\left(\lambda_n^4+K^6\right)+\frac{1}{36864}\lambda_n^4K^4+\frac{\lambda_n^4K^4}{1622016}\left(K^2-\lambda_n^2\right) \\ &\quad+\frac{\lambda_n^2K^2}{6488064}\left(\lambda_n^6-K^6\right)+\frac{\lambda_n^4K^4}{122683392}\left(K^4+\lambda_n^4\right) \\ &\quad-\frac{1}{69009408}\lambda_n^6K^6-\frac{1}{5096079360}\lambda_n^6K^8 \\ &\quad+\frac{\lambda_n^6K^6}{5096079360}\left(\lambda_n^2-K^2\right)+\frac{1}{369635622912}\lambda_n^8K^8+\cdots. \end{aligned} \tag{27}$$

## 3. Results and discussion

In this analytical description of electro-osmotic flow in a circular micro-channel, the governing parameter is $\Omega$ which represents the ratio of the diffusion time scale $\left(t_{\text{diff}} = \rho\Re^2/\mu\right)$ to the period of the applied electric field$(t_E = 1/\omega)$. Figs. 1–3 compare the time-periodic velocity profiles in a circular channel for two cases: (a) $\Omega = 30$ and (b) $\Omega = 300$. These two $\Omega$ values correspond to frequencies of 500 Hz and 5 kHz in a 100 μm channel. To illustrate the essential features of the velocity profile, a relatively large double layer thickness has been used, $\kappa = 6\times10^6\ \text{m}^{-1}$ (corresponding to a bulk ionic concentration $n_\infty = 10^{-6}$ M), and a uniform surface potential of $\zeta = 12.5$ mV was used (within the bounds imposed by the Debye–Huckel linearization). Also, in order to have a more realistic view on the problem, another double layer thickness, $\kappa = 2\times10^7\ \text{m}^{-1}$ has been examined.

Figs. 1–3 have been plotted by using $\kappa = 6\times10^6\ \text{m}^{-1}$. From Figs. 1 and 2, it is apparent that the application of the electrical body force results in a rapid acceleration of the fluid within the double layer. Fig. 1 shows the non-dimensional velocity profiles using sinusoidal wave, at $\Omega\theta = \omega t = \pi/2, \pi, 3\pi/2, 2\pi$ for two different $\Omega$ values. It is seen that applying high $\Omega$ values causes the fluid momentum not to have sufficient time to diffuse far into the bulk flow; hence the fluid within the double layer oscillates rapidly, while the bulk fluid remains almost stationary. Fig. 2 shows the non-dimensional velocity profiles using square wave, at $\Omega\theta = \omega t = \pi/2, \pi, 3\pi/2, 2\pi$ for two different $\Omega$ values. Their behaviors at high $\Omega$ values are like when sinusoidal wave is used; that is, at high $\Omega$ values, the bulk flow is not almost influenced by alternating electrical field. In this case, the oscillation amplitude of velocity is higher compared with the sinusoidal waveform. To illustrate the significant effects of some particular waveforms on the transient response of the bulk flow, Fig. 3(a) and (b) represent the channel midpoint velocities (i.e. velocity at $R = 0$) for $\Omega = 30$ and $\Omega = 300$, respectively. As shown in Fig. 3(a), a square wave excitation tends to produce higher velocities compared to the sinusoidal waveform. As $\Omega$ is increased, the initial positive impulsive velocity is observed for both waveforms, as illustrated in Fig. 3(b). As expected, the fluid excited by the square waveform exhibits higher instantaneous velocities, which lead to an increase in the number of cycles required to reach the time periodic quasi-steady state oscillation.

Fig. 4, that has been plotted using $\kappa = 2\times10^7\ \text{m}^{-1}$, illustrates the non-dimensional velocity distributions using sinusoidal and square waveforms at $\Omega\theta = \omega t = \pi/2, \pi, 3\pi/2, 2\pi$ for two different values of $\Omega$. Compared with Figs. 1 and 2, it is clear that an increase in $\kappa$ or a decrease in the Debye length results in an increase in the maximum velocity near the channel wall (at the same volumetric flow rate). Correspondingly, the EDL potential field falls off to zero more rapidly with distance, that is, the region influenced by the EDL is smaller.

Fig. 5 compares the near-wall velocity profiles at various times with the corresponding results given by Dutta and Beskok [11] in

$$V(R,\theta) = \frac{K^2 Z}{\pi I_0(K)} \sum_{n=1}^{\infty} \frac{J_0(\lambda_n R)\left(\int_0^1 J_0(\lambda_n \ell)\, I_0(K\ell)\, d\ell\right)\left(\lambda_n^2 \sin(\Omega\theta) - \Omega\cos(\Omega\theta) + \Omega\, e^{-\lambda_n^2\theta}\right)}{\left(\lambda_n^4 + \Omega^2\right) J_1^2(\lambda_n)}. \tag{24}$$

**Box I.**

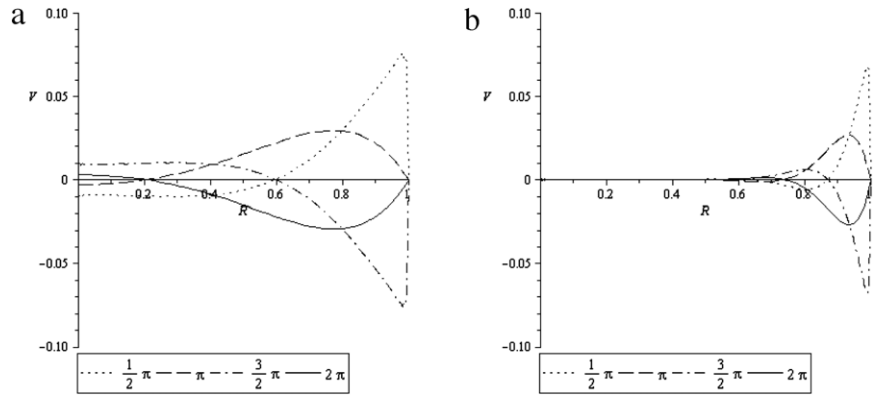


**Fig. 1.** Steady-state time periodic non-dimensional velocity profiles with $\kappa\Re = 300$, for one period ($0 < \Omega\theta \leq 2\pi$) of the sinusoidal waveform at (a) $\Omega = 30$ and (b) $\Omega = 300$.

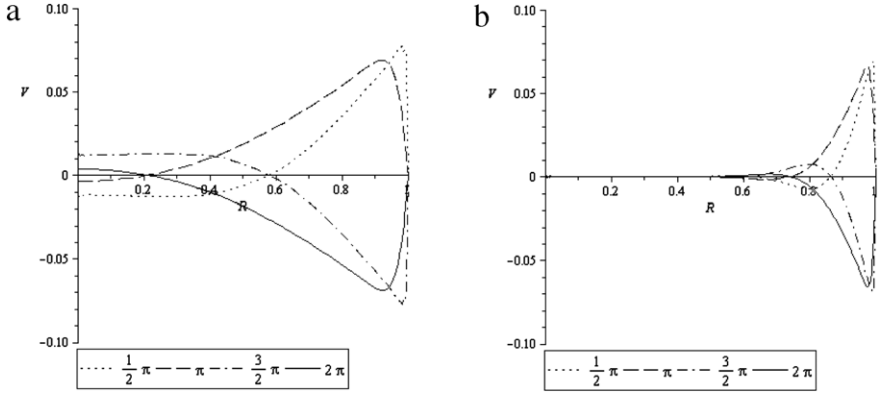


**Fig. 2.** Steady-state time periodic non-dimensional velocity profiles with $\kappa\Re = 300$, for one period ($0 < \Omega\theta \leq 2\pi$) of the square waveform at (a) $\Omega = 30$ and (b) $\Omega = 300$.

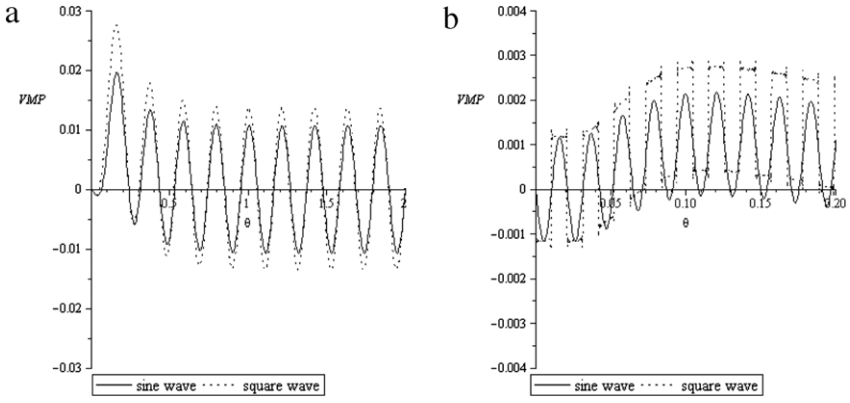


**Fig. 3.** Transient stage non-dimensional velocity with $\kappa\Re = 300$, at the channel midpoint for impulsively started flows using sinusoidal and square waveforms at (a) $\Omega = 30$ and (b) $\Omega = 300$.

a two-dimensional straight channel. The distance from the wall, where the normalized electro-osmotic potential reaches 1% of its base value, is defined as $\delta_{99}$. With the EDL thickness $\lambda = 320$ nm and the frequency $\Omega = 6250$ (equivalent to $10^5$ Hz), the effective EDL thickness is $\delta_{99} \simeq 0.03$, or according to the non-dimensionalization, is $\delta_{99} = 4.6875\lambda$. As can be seen, the velocity field within the EDL is similar for identical applied electric field.

In this study, an analytical analysis based on the linearized Poisson–Boltzmann equation has been developed for liquid flow in a circular micro-channel induced by unsteady applied electric fields.

In the case where the diffusion time scale is much greater than the oscillation period (high $\Omega$), there is insufficient time for the fluid momentum to diffuse far into the bulk flow and thus,

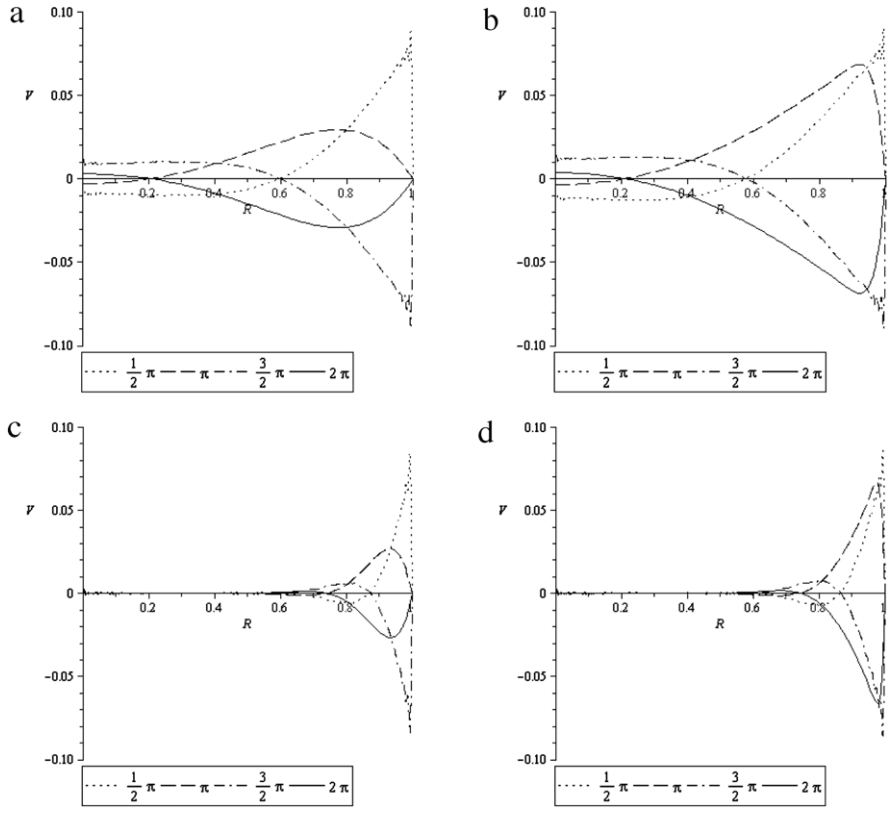


**Fig. 4.** Steady-state time periodic non-dimensional velocity profiles with $\kappa\Re = 1000$, for one period ($0 < \Omega\theta \leq 2\pi$) of the sinusoidal and square waveforms at (a) $\Omega = 30$ (sine wave), (b) $\Omega = 30$ (square wave), (c) $\Omega = 300$ (sine wave), and (d) $\Omega = 300$ (square wave).

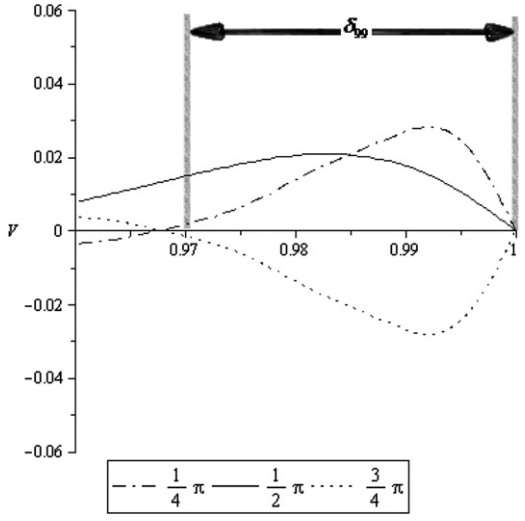


**Fig. 5.** Near-wall velocity distribution for $\kappa\Re = 156.25$ at $\Omega = 6250$ at various times.

while the fluid within the double layer oscillates rapidly, the bulk fluid remains almost stationary. But at a lower $\Omega$ value ($\Omega = 30$), there is more time for momentum diffusion from the double layer; however the bulk fluid still lags behind the flow in the double layer. Extrapolating from these results, when $\Omega < 1$, such that momentum diffusion is faster than the period of oscillation, the plug like velocity profile characteristic of steady-state electro-osmotic flow would be expected at all times.

The finite time required for momentum diffusion will inevitably result in some degree of phase shift between the applied electric field and the flow response in the channel. From figures represented here, however, it is apparent that within the limit of $\Omega > 1$, this phase shift is significantly different in the double layer region than in the bulk flow. It is apparent that the response of the fluid within the double layer to the AC field is essentially immediate; however, the bulk liquid lags behind the applied field by a phase shift depending on the $\Omega$ value. Additionally, while the velocity in the double layer reaches its steady state oscillation almost immediately, the bulk flow requires a period before the transient effects are dissipated. In Eq. (24), the out-of-phase cosine term $\Omega\cos(\Omega\theta)$ is proportionally scaled by $\Omega$. A similar term ($\Omega\cos(m\Omega\theta)$) also exists in Eq. (26). Thus as expected, when $\Omega$ is increased, the phase shift for both the double layer and bulk flow velocities is increased as is the number of cycles required to reach the steady state. It is interesting to note the net positive velocity at the channel midpoint within the transient period before decaying into the steady state behavior. This is a result of the initial positive impulse given to the system when the electric field is first applied and is reflected by the exponential term in Eq. (24) (and similarly in (26)). The transient oscillations are observed to decay at an exponential rate, as expected from the transient term. Similar to the out-of-phase cosine term, this exponential term is also proportionally scaled by the non-dimensional frequency, suggesting that the effect of the initial impulse becomes more significant with increasing $\Omega$. A square wave excitation tends to produce higher velocities than the sinusoidal wave form.

## References

[1] S. Kandlikar, S. Garimella, D. Li, S. Colin, M.R. King, Heat Transfer and Fluid Flow in Minichannels and Microchannels, Elsevier, 2006.
[2] J.L. Anderson, Effect of nonuniform zeta potential on particle movement in electric fields, J. Colloid Interface Sci. 105 (1985) 45–54.
[3] A. Ajdari, Electroosmosis on inhomogeneously charged surfaces, Phys. Rev. Lett. 75 (1995) 755–758.

[4] M. Wang, S. Chen, Electroosmosis in homogeneously charged micro- and nanoscale random porous media, J. Colloid Interface Sci. 314 (2007) 264–273.
[5] M. Wang, Q. Kang, H. Viswanathan, B.A. Robinson, Modeling of electro-osmosis of dilute electrolyte solutions in silica microporous media, J. Geophys. Res. 115 (2010) B10205.
[6] P. Dutta, A. Beskok, Analytical solution of combined electroosmotic/pressure driven flows in two-dimensional straight channels: finite Debye layer effects, Anal. Chem. 73 (2001) 1979–1986.
[7] S. Arulanandam, D. Li, Liquid transport in rectangular microchannels by electroosmotic pumping, Colloids Surf. A (2000) 89–102.
[8] C.Y. Soong, S.H. Wang, Theoretical analysis of electrokinetic flow and heat transfer in a microchannel under asymmetric boundary conditions, J. Colloid Interface Sci. 265 (2003) 202–213.
[9] Y. Kang, C. Yang, X. Huang, Dynamic aspects of electroosmotic flow in a cylindrical microcapillary, Internat. J. Engrg. Sci. 40 (2002) 2203–2221.
[10] M. Wang, Q. Kang, Modeling elctrokinetic flows in microchannels using coupled lattice Boltzmann methods, J. Comput. Phys. 229 (2010) 728–744.
[11] P. Dutta, A. Beskok, Analytical solution of time periodic electroosmotic flows: analogies to stokes second problem, Anal. Chem. 73 (2001) 5097–5102.
[12] O. Soderman, B. Jonsson, Electro-osmosis: velocity profiles in different geometries with both temporal and spatial resolution, J. Chem. Phys. 105 (1996) 10300–10311.
[13] D. Erickson, D. Li, Analysis of AC electroosmotic flows in a rectangular microchannel, Langmuir 19 (2003) 5421–5430.
[14] N.G. Green, A. Ramos, A. Gonzalez, H. Morgan, A. Castellanos, Fluid flow induced by non-uniform AC electric fields in electrolytes on microelectrodes I: experimental measurements, Phys. Rev. E 61 (2000) 4011–4018.
[15] A. Gonzalez, A. Ramos, N.G. Green, A. Castellanos, H. Morgan, Fluid flow induced by non-uniform AC electric fields in electrolytes on microelectrodes II: a linear double layer analysis, Phys. Rev. E 61 (2000) 4019–4028.
[16] A.B.D. Brown, C.G. Smith, A.R. Rennie, Pumping of water with an AC electric field applied to asymmetric pairs of microelectrodes, Phys. Rev. E 63 (2002) 016305 1–8.
[17] V. Studer, A. Pepin, Y. Chen, A. Ajdari, Fabrication of microfluidic devices for AC electrokinetic fluid pumping, Microelectron. Eng. 61–62 (2002) 915–920.
[18] N.T. Nguyen, S.T. Wereley, Fundamentals and Applications of Microfluidics, ARTECH HOUSE, 2006.
[19] P. Tabeling, Introduction to Microfluidics, Oxford University Press, 2005.
[20] R. Haberman, Elementary Applied Partial Differential Equations, Prentice Hall, 1987.